Supporting information

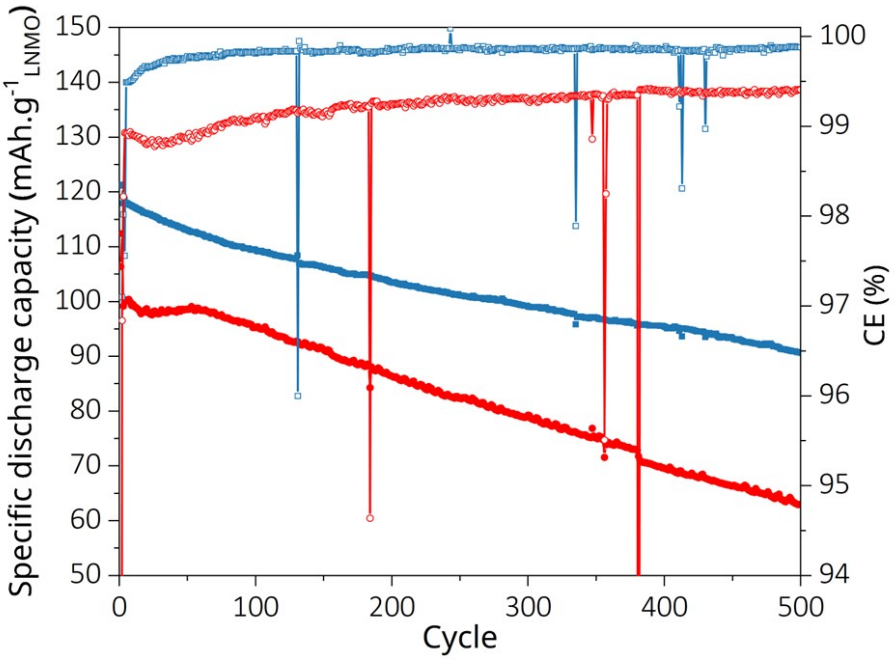

Figure S1: Long term cycling of graphite||LNMO cell using the carbonate-based (blue) and the SL-based (red) electrolyte. Artifacts in the curves are due to interruptions in the potentiostat measurements.

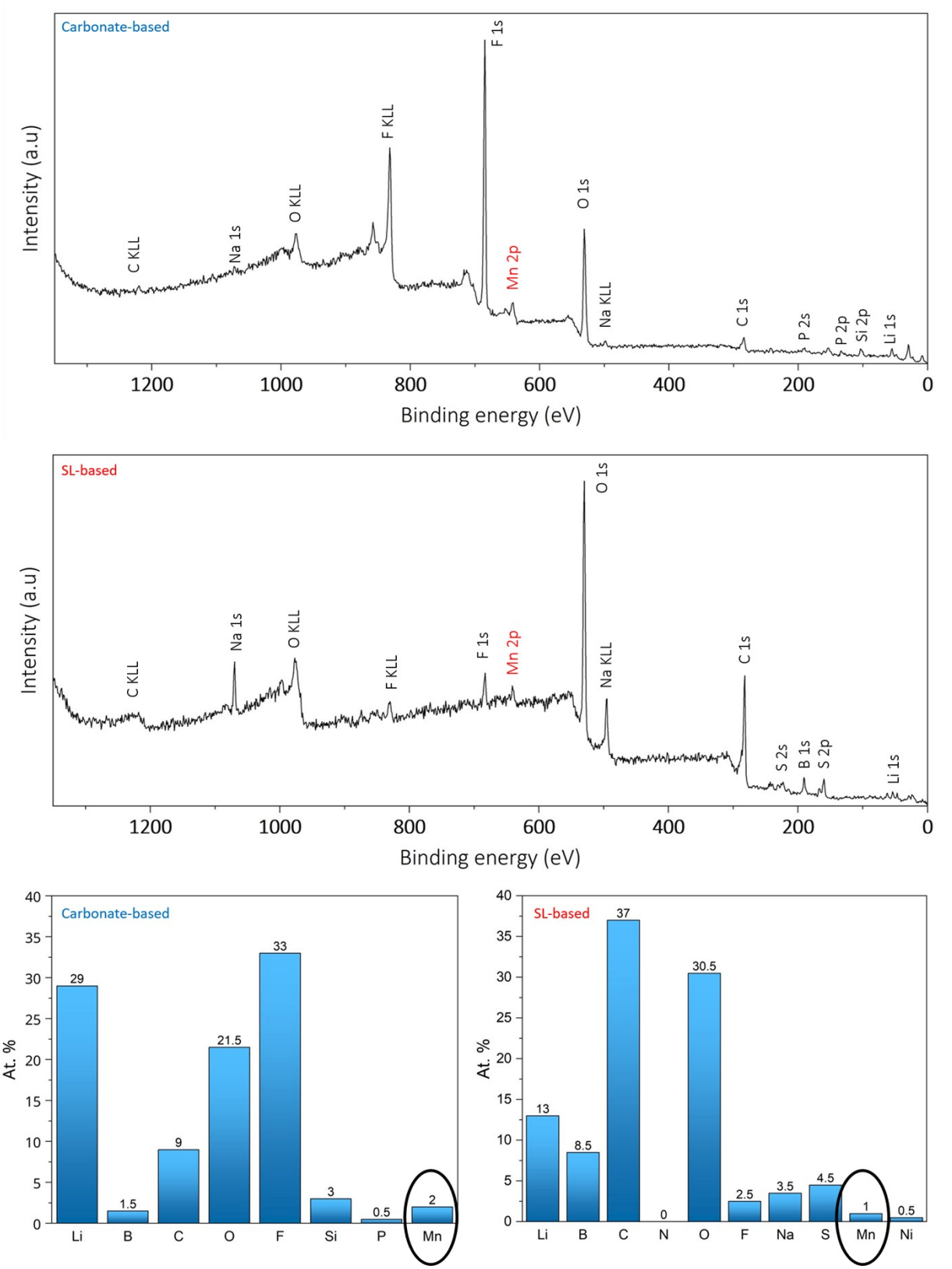

Figure S2: Survey XPS spectra of graphite electrodes collected after 100 discharges with the carbonate-based electrolyte (top) and the SL-based electrolyte (middle) and elemental analysis (bottom). Data collected after 14 min of Ar+ sputtering.

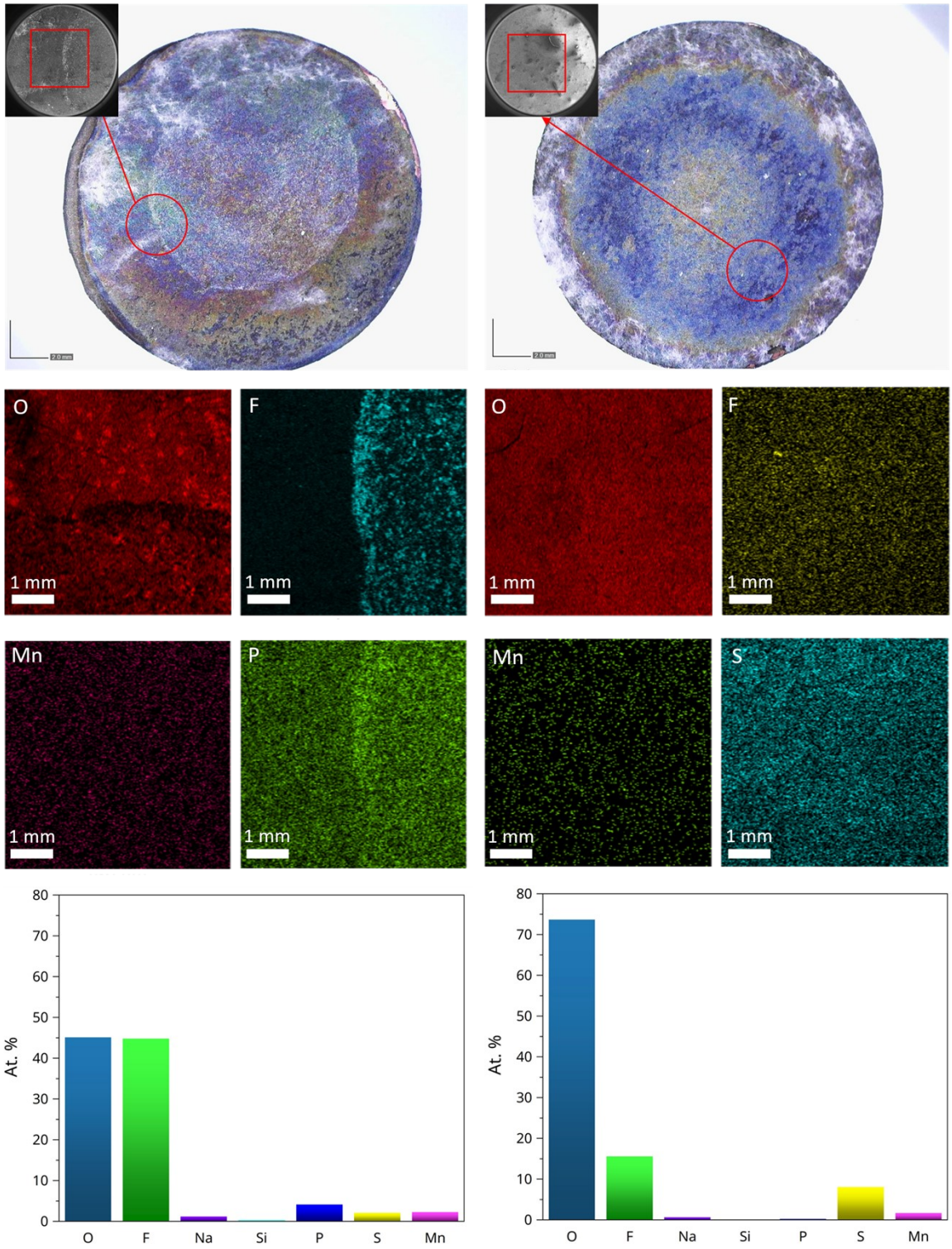

Figure S3: EDX analysis of graphite electrodes cycled for 150 discharges with the carbonate-based (left) and the SL-based electrolyte (right).

Low magnification pictures of the electrodes were taken with a portable visible-light microscope after 150 discharges (Figure S3). Both graphite electrodes exhibited characteristic colour variations ranging from blue to bronze and gold, which correspond to different degrees of graphite lithiation: blue indicates low lithiation, bronze intermediate, and gold full lithiation.[1,2] The electrode cycled with the carbonate-based electrolyte displayed a broader distribution of bronze and gold regions, suggesting a greater amount of lithium trapped in the graphite at the end of discharge compared to the electrode cycled with the SL-based electrolyte. Additionally, a distinct greyish circular feature was observed at the centre of the graphite electrode cycled in the carbonate-based electrolyte. Energy-dispersive X-ray spectroscopy (EDX) identified this region as being rich in fluorine (Figure S3), pointing to the accumulation of LiF crystals or insoluble fluorine-rich species. This localised LiF formation likely occurs in the central area of the electrode where current density may be higher due to pressure heterogeneity, promoting electrolyte decomposition and salt-derived byproduct precipitation.

Table S1: Refine lattice parameter and FWHM for pristine LNMO and LNMO after 150 cycles vs. graphite using the carbonate- and SL-based electrolytes.

	Pristine LNMO	Carbonate-based el.	SL-based el.
a (Å)	8.1819(2)	8.1601(2)	8.1488(2)
FWHM (°)	0.06073	0.07246	0.08109

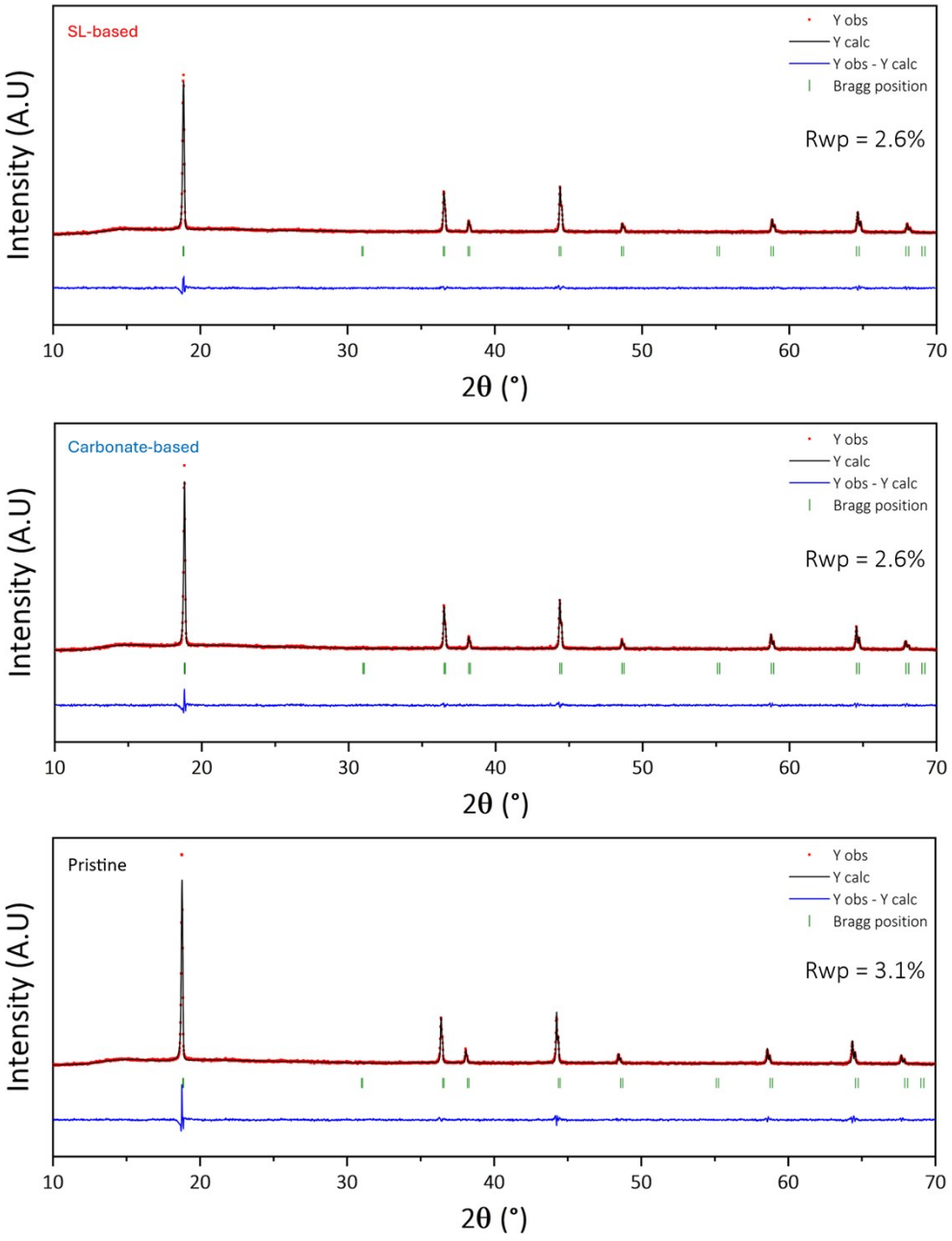

Figure S4: Fitted diffractogram for pristine LNMO and LNMO after 150 cycles vs. graphite using the carbonate- and SL-based electrolytes.

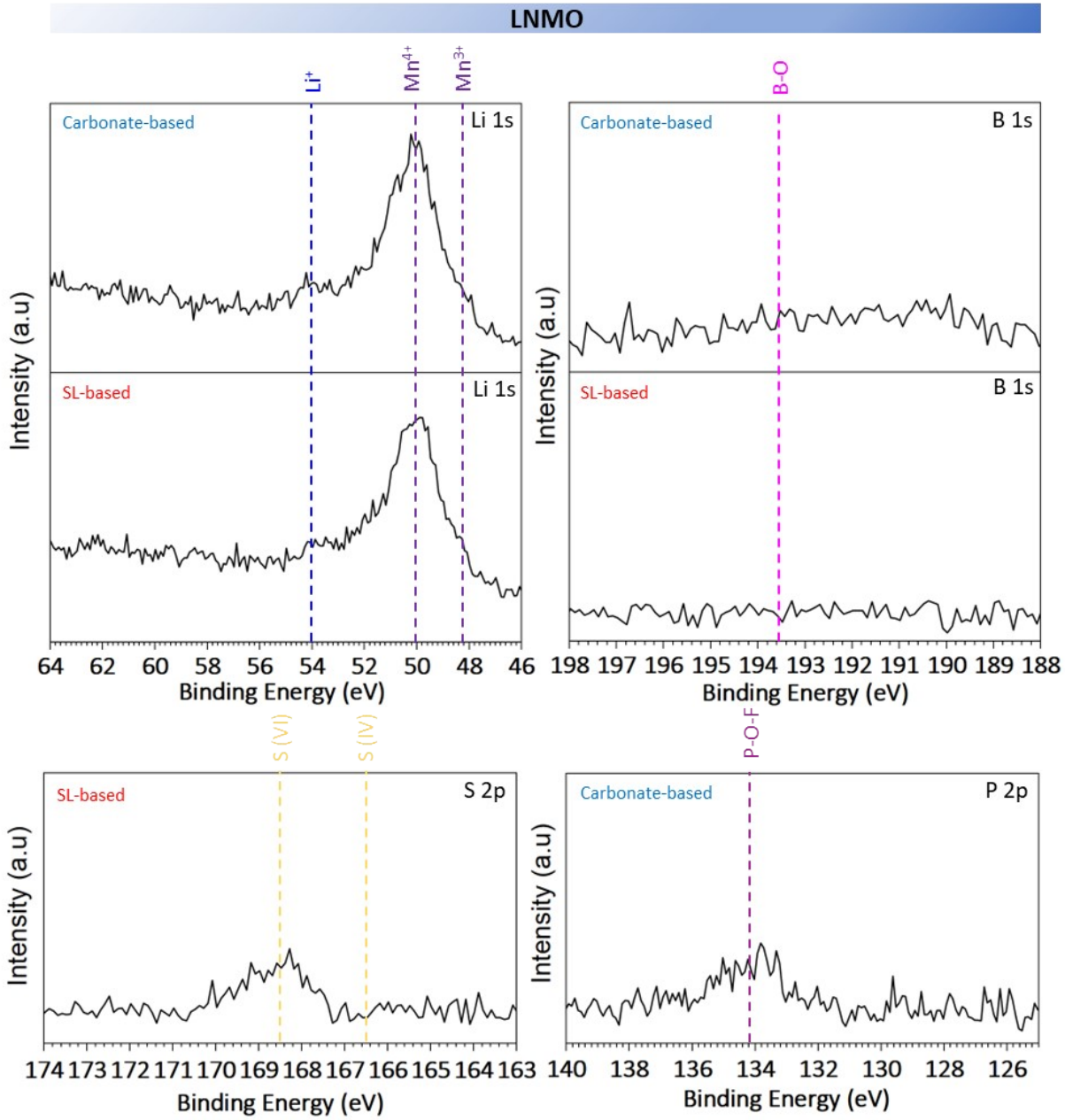

Figure S5: XPS analysis of Li 1s, B 1s, S 2p and P 2p for graphite electrodes collected after 100 discharges with the carbonate-based electrolyte or the SL-based electrolyte.

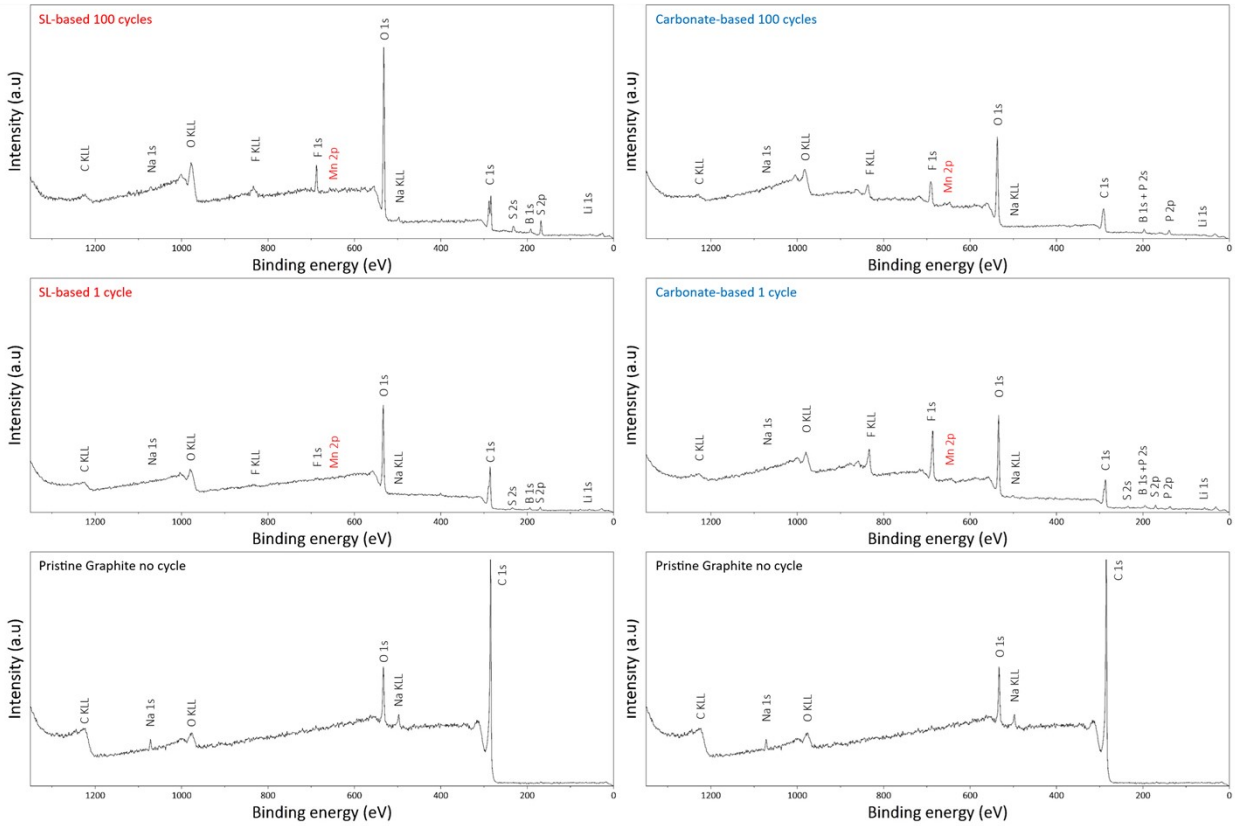

Figure S6: Survey XPS spectra of pristine and cycled graphite electrodes collected after 1 and 100 discharges with the carbonate-based electrolyte and the SL-based electrolyte.

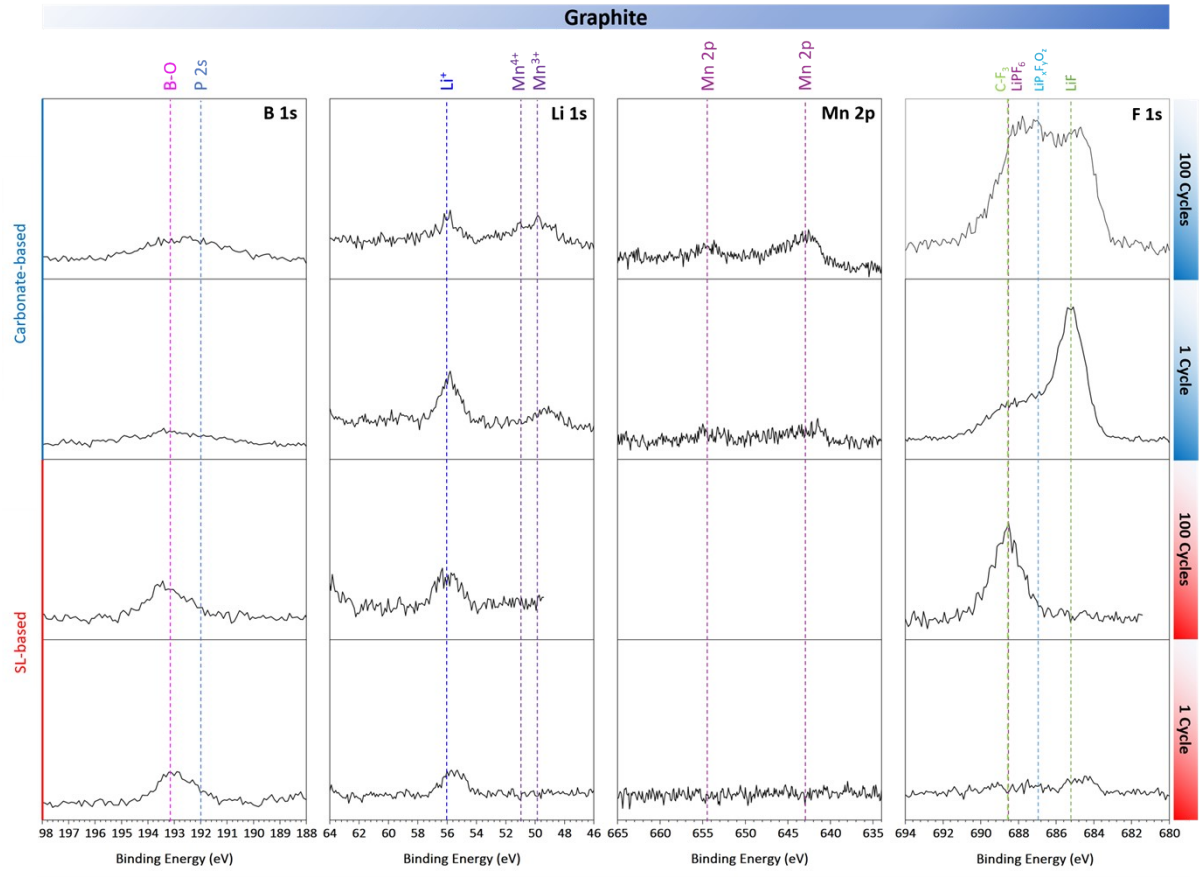

Figure S7: XPS analysis of B 1s, Li 1s, Mn 2p and F 1s for graphite electrodes collected after 1 and 100 discharges with the carbonate-based electrolyte or the SL-based electrolyte.

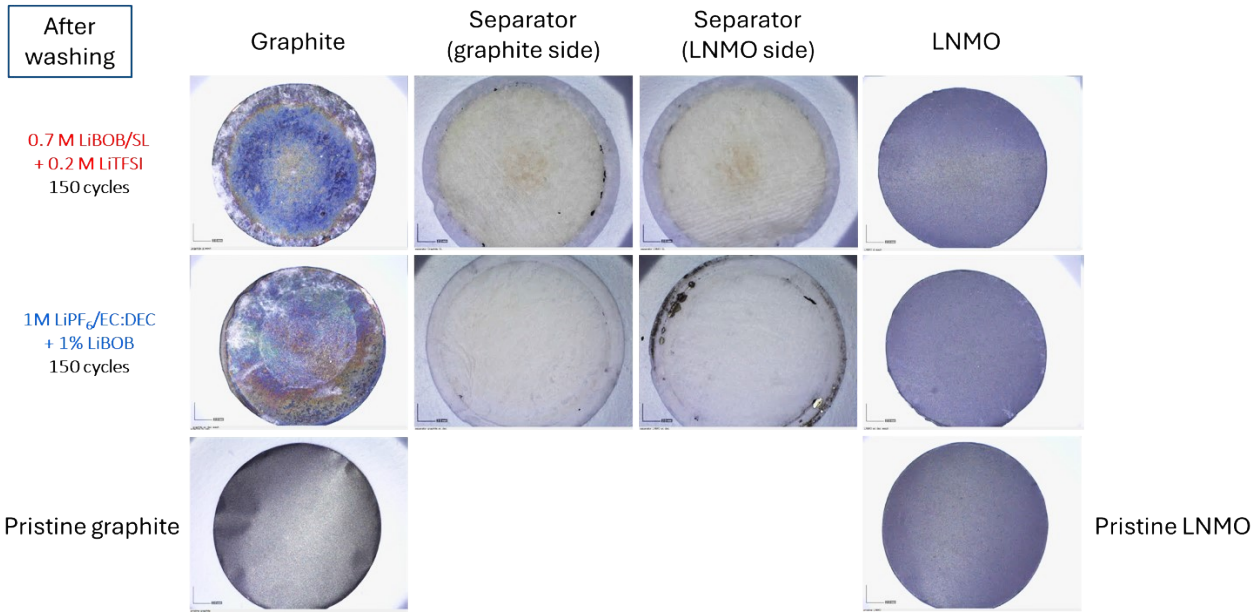

Figure S8: LNMO electrode, graphite electrode and both sides of the separator after 150 discharges using carbonate-based or SL-based electrolyte. Pristine graphite and LNMO electrode.

The separator from the cell cycled with the SL-based electrolyte exhibits a pronounced orangish coloration on both sides (Figure S8), consistent with the accumulation of soluble decomposition byproducts in the electrolyte[3]. This visual indication supports the presence of extensive electrolyte decomposition product. In contrast, the separator from the carbonate-based electrolyte cell remains mostly white, potentially suggesting a lower degree of soluble species and better interphase stability under these cycling conditions. Notably, both electrolytes seem prone to releasing oxidation products into the electrolyte, but this effect appears more pronounced with the SL-based composition.[4,5].

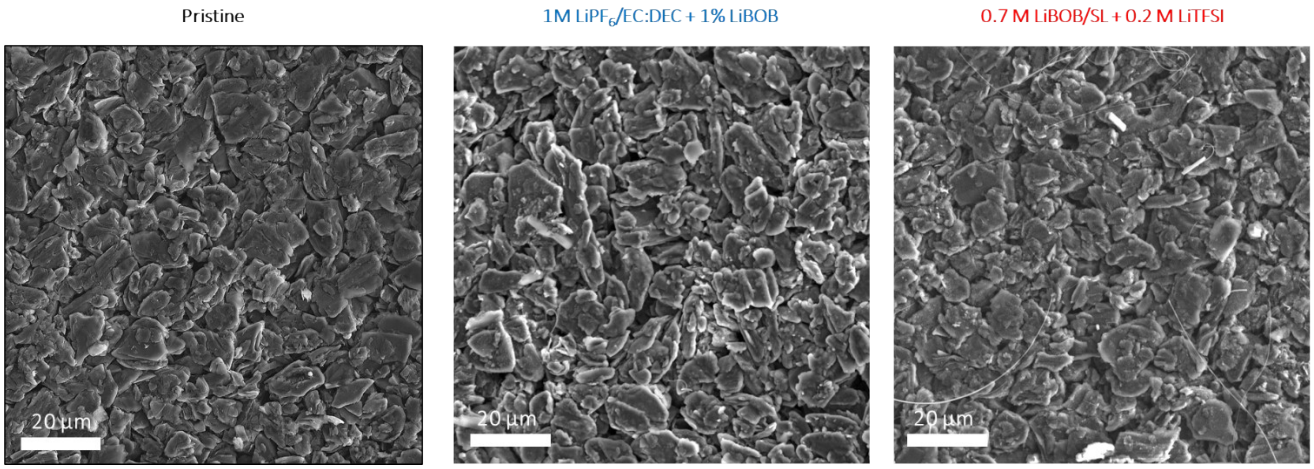

Figure S 9: SEM images of the pristine graphite electrode (left), graphite electrode after 150 discharges with the carbonate-based (centre) and the SL-based electrolyte (right).

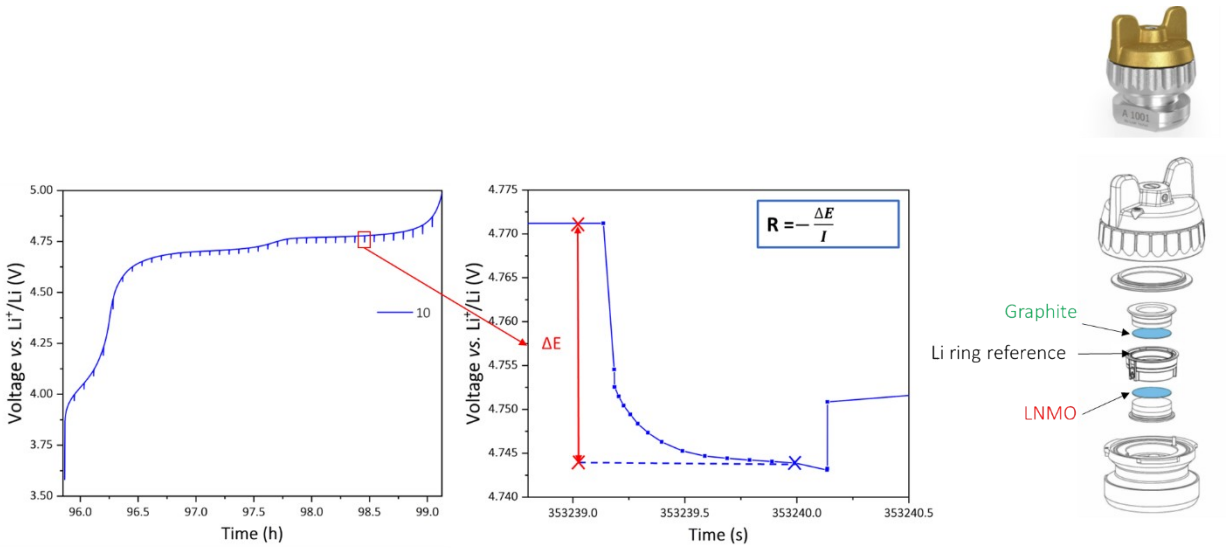

Figure S10: Example of ICI measurement (left). Focus on one current interruption (middle). Schematic of the Pat cell use for the ICI measurements (right).

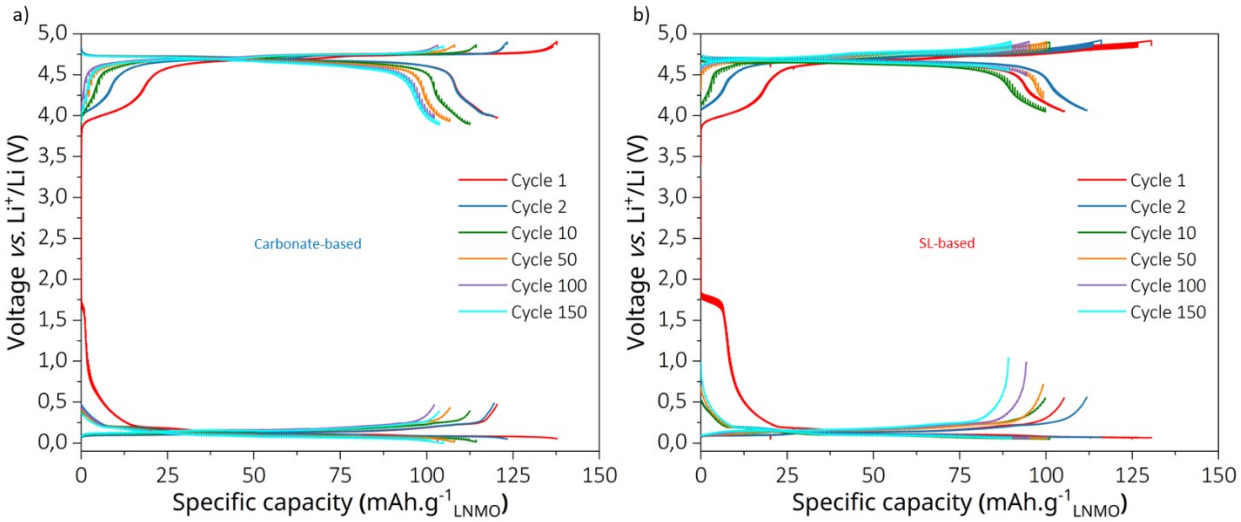

Figure S11: Galvanostatic profile of the three-electrode graphite||LNMO cells used to track the IR by ICI in Figure 4.

```python
import numpy as np
import pandas as pd
import matplotlib.pyplot as plt
import os
from matplotlib.lines import Line2D
from pathlib import Path

# Parameters
FILENAME = "Bat732_G_LNMO_1M_LiPF6_EC_DEC_1%LiBOB_ICI_3E_PAT_cell_ref_Li_ring_C11.txt"
MASS = 26.71  # Mass of the active material in mg

# State constants
REST_STATE = 0
DISCHARGE_STATE = 1
CHARGE_STATE = 2

def load_and_process_data(filename, mass):
    """Load and process the battery data."""
    data = pd.read_csv(filename, delimiter='\t', header=0, decimal=',').to_numpy()
    data = data.astype(float)

    cycle = data[:, 0]
    Qd = data[:, 1] * (1e3 / mass)  # Discharge capacity (Ah)
    cQ = data[:, 2] * (1e3 / mass)  # Charge capacity (Ah)
    i = data[:, 3] / 1000           # Current (A)
    Ewe = data[:, 4]                # Voltage We (V)
    Ece = data[:, 5]                # Voltage Ce (V)
    t = data[:, 6]                  # Time (s)

    adj_Q = Qd - cQ

    return cycle, Qd, cQ, i, Ewe, Ece, t, adj_Q

def determine_states(current):
    """Determine states based on current values."""
    state = np.zeros(len(current))
    state[current == 0] = REST_STATE
    state[current < 0] = DISCHARGE_STATE
    state[current > 0] = CHARGE_STATE
    return state

def find_rest_transitions(state, time_array):
    """Find rest state transitions and return relevant indices."""
    transitions = []
```

```
    for i in range(1, len(state)):
        if state[i - 1] == REST_STATE and state[i] != REST_STATE:
            if i + 2 < len(time_array):
                transitions.append({
                    'index': i + 2,
                    'time': time_array[i + 2],
                    'next_state': state[i]
                })

    return transitions

def calculate_resistances(transitions, Ewe, Ece, current, cycle, adj_Q, Qd, cQ):
    """Calculate resistances and organize data."""
    n_transitions = len(transitions)

    # Initialize arrays
    arrays = {
        'Rwe': np.zeros(n_transitions),
        'Rce': np.zeros(n_transitions),
        'new_Cap': np.zeros(n_transitions),
        'new_c': np.zeros(n_transitions),
        'new_Ewe': np.zeros(n_transitions),
        'new_Ece': np.zeros(n_transitions),
        'new_Qd': np.zeros(n_transitions),
        'new_cQ': np.zeros(n_transitions),
        'is_discharge': np.zeros(n_transitions, dtype=bool)
    }

    for i, transition in enumerate(transitions):
        idx = transition['index']
        arrays['Rwe'][i] = (Ewe[idx] - Ewe[idx - 5]) / current[idx]
        arrays['Rce'][i] = abs((Ece[idx] - Ece[idx - 5]) / current[idx])
        arrays['new_Cap'][i] = adj_Q[idx]
        arrays['new_Ewe'][i] = Ewe[idx]
        arrays['new_Ece'][i] = Ece[idx]
        arrays['new_c'][i] = cycle[idx]
        arrays['new_Qd'][i] = Qd[idx]
        arrays['new_cQ'][i] = cQ[idx]
        arrays['is_discharge'][i] = (transition['next_state'] == DISCHARGE_STATE)

    return arrays
```

Figure S12: Extract of the Python code used to calculate the IR.

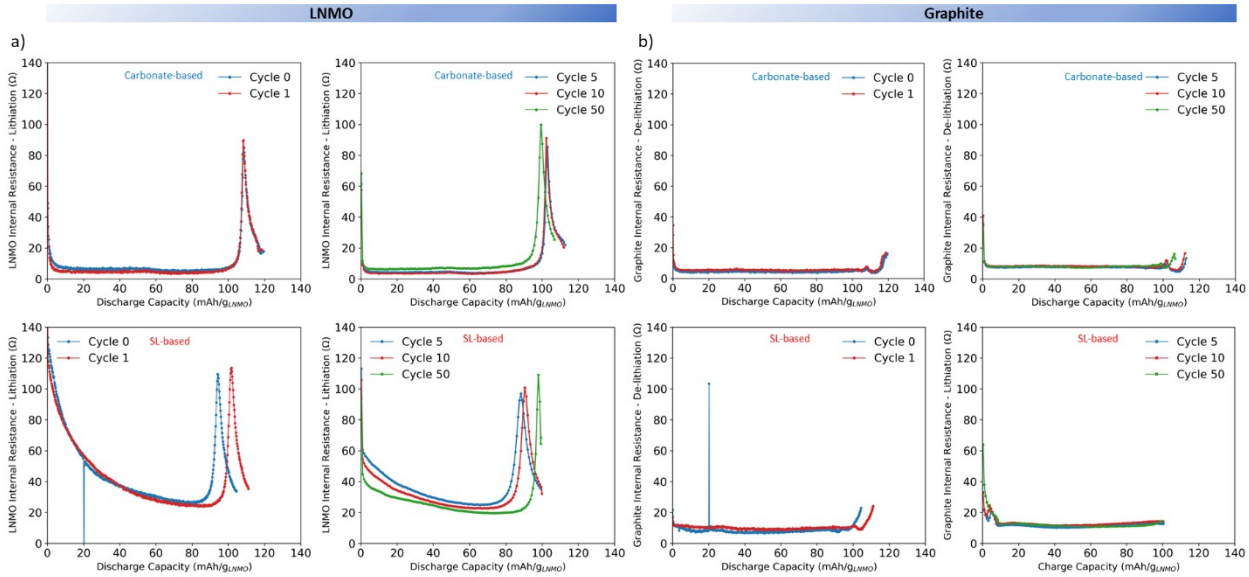

Figure S13: Internal resistance tracking during discharge in three-electrode cells using either the carbonate-based or SL-based electrolyte, shown for a) the LNMO electrode and b) the graphite electrode.

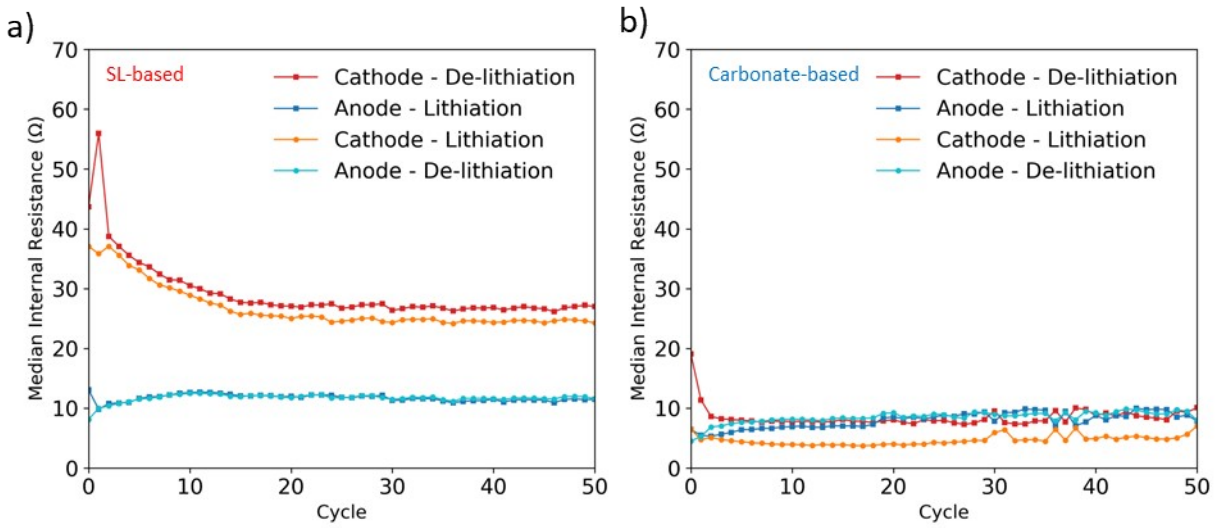

Figure S14: Median internal resistance of the graphite and LNMO electrode during Lithiation and de-Lithiation with a) the carbonate-based electrolyte and b) the SL-based electrolyte.

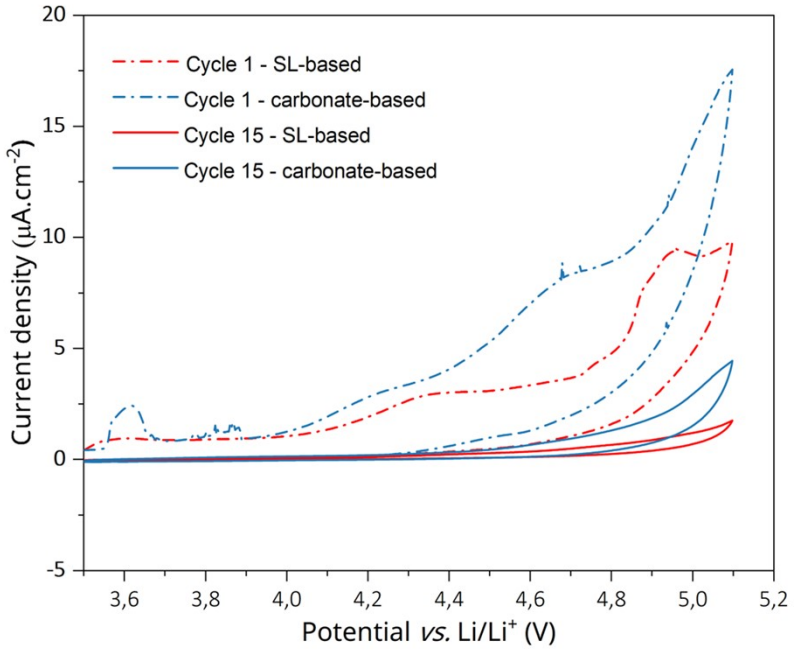

Figure S15: Cyclic voltammetry of Li||Al cells after 1 cycle and 15 cycles using the SL-based electrolyte and the carbonate-based electrolyte.

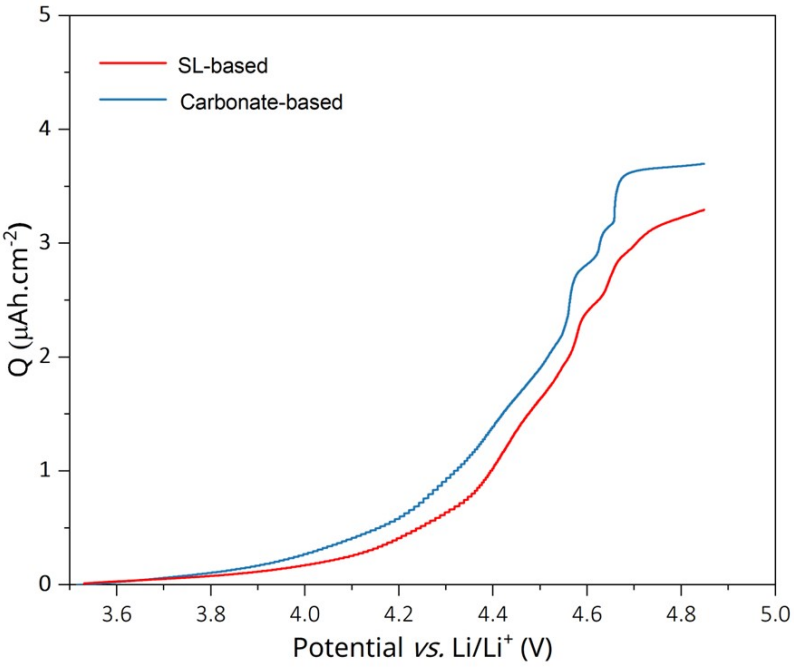

Figure S16: SCPV of Li||Al cells during 1 charge using the SL-based electrolyte and the carbonate-based electrolyte.

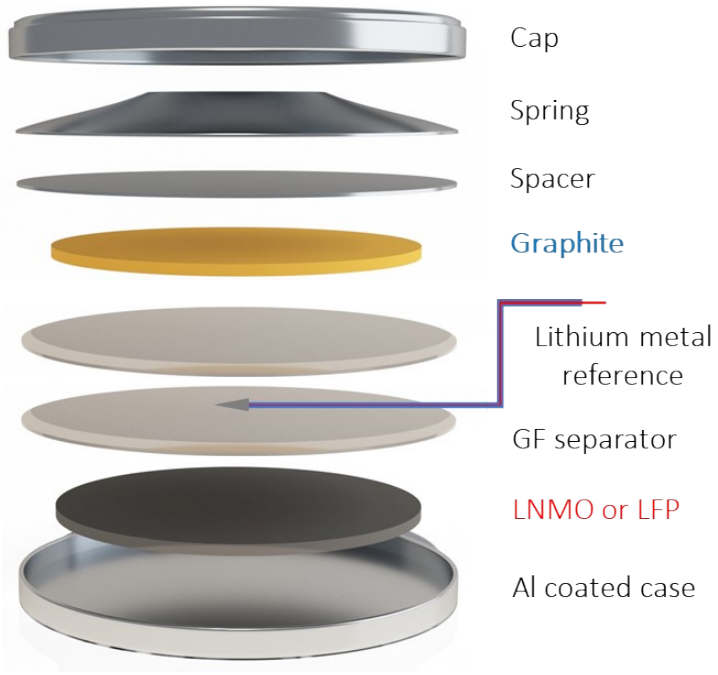

Figure S17: Schematic of the three-electrode coin cells used for the graphite-limited cells.

References

1 Y. Chen, K. H. Chen, A. J. Sanchez, E. Kazyak, V. Goel, Y. Gorlin, J. Christensen, K. Thornton and N. P. Dasgupta, *J Mater Chem A Mater*, 2021, **9**, 23522–23536.

2 A. Shellikeri, V. Watson, D. Adams, E. E. Kalu, J. A. Read, T. R. Jow, J. S. Zheng and J. P. Zheng, *J Electrochem Soc*, 2017, **164**, A3914–A3924.

3 S. Sattar, T. Statheros, A. Raza, Q. Kellner, Y. Yu, R. Bhagat, A. J. Roberts and Y. Guo, *Sensors*, DOI:10.3390/s24237686.

4 B. Aktekin, M. J. Lacey, T. Nordh, R. Younesi, C. Tengstedt, W. Zipprich, D. Brandell and K. Edström, *Journal of Physical Chemistry C*, 2018, **122**, 11234–11248.

5 R. Dedryvère, D. Foix, S. Franger, S. Patoux, L. Daniel and D. Gonbeau, *Journal of Physical Chemistry C*, 2010, **114**, 10999–11008.